Available online at www.sciencedirect.com
SCIENCE DIRECT
Journal of Membrane Science 279 (2006) 635–644
journal of MEMBRANE SCIENCE
www.elsevier.com/locate/memsci

Comparative behaviour of hydrophilic membranes in the pervaporative dehydration of cyclohexane

P. Gómez [a], M.C. Daviou [b,1], R. Ibáñez [a], A.M. Eliceche [a], I. Ortiz [a,*]

[a] *Departamento de Ingeniería Química, ETSIIT, Universidad de Cantabria, Avda. de los Castros s/n, 39005 Santander, Spain*
[b] *Departamento de Ingeniería Química, Universidad Nacional del Sur-PLAPIQUI, Camino La Carrindanga km 7, 8000 Bahía Blanca, Argentina*

Received 9 September 2005; received in revised form 29 November 2005; accepted 25 December 2005
Available online 14 February 2006

Abstract

This work focuses on the performance analysis of several commercial membranes, provided by Celfa (VP-31, VP-43 and CF-23) and Sulzer (Pervap2201 and Pervap2201D) companies, as well as some tailor made sulfonated poly(ether ether ketone) (SPEEK) membranes, in the pervaporative dehydration of cyclohexane which is commonly employed as solvent in the synthetic rubber manufacture. Water permeate fluxes in the range of 13–250 mg/m^2 min and satisfactory selectivity values were observed at very low water contents in the feed (below 90 mg/kg). A mathematical model based on the solution-diffusion theory is also presented, taking into account the mass transfer resistance offered by the fluid layer and the membrane itself, supported with experimental data obtained in a bench-scale radial flow pervaporation cell. Permeability values of the studied membranes resulted in the range of 3.2×10^{-11} to 2.3×10^{-9} m^2/s.

Keywords: Pervaporation; Dehydration; Cyclohexane; Commercial membranes; SPEEK; SPEEK/PES

1. Introduction

Drying of solvents and raw materials is a crucial step in many industrial processes, as in the production of ethanol and other important organic compounds, or in the purification of raw materials, as it is the case in the synthetic rubber industry. The catalytic process developed in the manufacture of different elastomers based on styrene consists of an anionic polymerization reaction in solution, where *n*-butyl lithium is used as the initiator of the process. The high influence of impurities (mainly polar compounds) in the extremely sensitive and complex catalytic reaction [1] turns the preliminary purification of raw materials into a critical point in the production process. The high affinity of this *n*-butyl lithium initiator to polar impurities results in its excessive consumption and undesirable delay in the reaction kinetics. Consequently, high-performance purification operations are employed to condition the raw materials, styrene and butadiene, as well as the employed solvent, cyclohexane.

After reaction, cyclohexane is separated from the polymer by steam-stripping, recovered and pumped to a distillation purification column where a small fraction of fresh cyclohexane is also added. Owing to the amount of impurities coming from the polymerization reaction, typically between 0.053 and 0.099 kg/m^3 [2], together with water dissolved by the solvent, a high-efficiency distillation operation is required.

Pervaporation (PV) is presented in the literature as an economic alternative for reducing energy costs when integrated in a hybrid pervaporation–distillation process [3,4]. This process is especially appropriate in azeotropic and close boiling point mixture separations and in the removal of small amounts of water from organics [5]. The PV technology has received relatively little attention in dehydration applications at low water concentration values [6,7], although removal of diluted organics from wastewater is well known [8,9]. The low permeability of the membrane polymers in the range of low water concentration together with the chemical resistance required to the organic compounds result in the need of a systematic search of the material with suitable properties for these applications.

The aim of this work is the study of the permeation behaviour of water/cyclohexane mixtures through hydrophilic membranes,

* Corresponding author. Tel.: +34 942 201585; fax: +34 942 201591.
E-mail address: ortizi@unican.es (I. Ortiz).
[1] Tel.: +54 291 4861700; fax: +54 291 4861600.

0376-7388/$ – see front matter © 2006 Elsevier B.V. All rights reserved.
doi:10.1016/j.memsci.2005.12.061

in order to obtain information for future process design. Two different types of membranes have been selected for this purpose (i) commercial materials commonly employed in the dehydration of organic mixtures and (ii) other promising materials, owing to its hydrophilic character, for dehydration applications and manufactured individually in the laboratory. Bench-scale tests were performed in the laboratory using a radial flow membrane cell and working in the range of water concentration in feed from 90 to 5 mg/kg. The influence of the membrane permeability, on the mass transport kinetics was analysed with the support of an equation-oriented simulation software. This tool allows the estimation of the relative importance of the boundary layer and membrane resistances in the process.

2. Theoretical model of the pervaporation process

The resistance-in-series model has been widely used by many authors in order to describe the mass transport through a dense homogenous polymeric membrane (see Fig. 1). As it is well described in literature [10,11], mass transport from the feed to the permeate side occurs following several steps that are analysed in this section.

2.1. Mass transport through the liquid boundary layer

Assuming low water concentration in the feed (from 90 to 10 mg/kg), constant solute diffusion coefficient in the solvent, and negligible convective flux (low back diffusion gradient), water flux through the liquid boundary layer results in,

$$J_w = k_l(C^b_{w,0} - C^b_{w,\delta}) \quad (1)$$

where the mass transfer coefficient in the liquid film, k_l, is calculated as a function of the Sherwood, Schmidt and Reynolds dimensionless numbers, through well-known correlations [10].

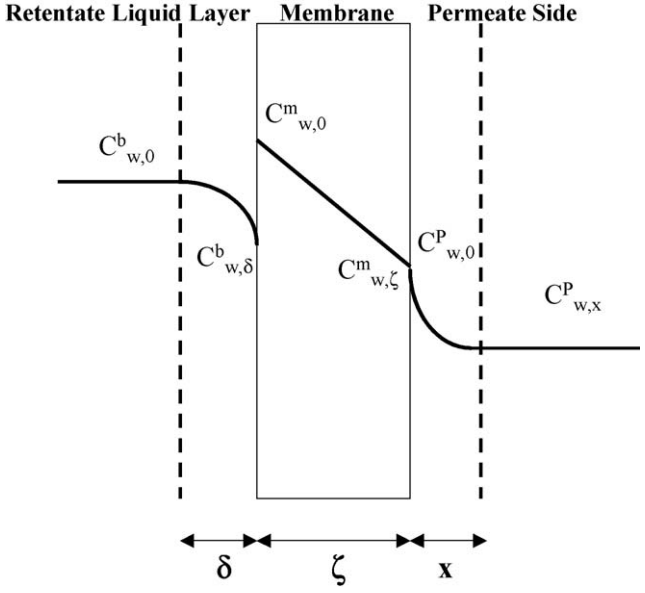

Fig. 1. Mass transport mechanism in a pervaporation process.

2.2. Sorption, diffusion through the dense top layer and desorption

Assuming thermodynamic equilibrium at the liquid/membrane interface, the concentration at the membrane surface, $C^m_{w,0}$, can be calculated from the liquid side composition, $C^b_{w,\delta}$ as follows [12]:

$$C^m_{w,0} = \frac{\gamma^b_{w,\delta}}{\gamma^m_{w,0}} C^b_{w,\delta} = K_{w,0} C^b_{w,\delta} \quad (2)$$

where, a sorption constant $K_{w,0}$ can be expressed as the activity coefficient ratio at the liquid and the membrane surface.

In addition, since desorbed molecules are continuously evaporated because of the low vacuum pressure applied in the permeate side, similar expressions can be applied to describe the desorption phenomena.

$$C^m_{w,\zeta} = \frac{\gamma^p_{w,0}}{\gamma^m_{w,\zeta}} C^p_{w,0} = K_{w,\zeta} C^p_{w,0} \quad (3)$$

where $K_{w,\zeta}$ is the desorption constant, and the water composition at the membrane/vapour interface is defined by $C^m_{w,\zeta}$, which is the concentration within the membrane at the permeate side, and $C^p_{w,0}$, that is the vapour concentration at the permeate side.

Fick's first law commonly describes diffusion through the membrane top layer. In this equation, membrane diffusivities of those components that permeate are expressed as a function of their concentrations in the membrane. Thus, diffusion of water can be described as follows:

$$D_{w,m} = D^0_{w,m} \exp(\tau_{w,w} C^m_w + \tau_{w,c} C^m_c) \quad (4)$$

Being $\tau_{w,w}$ the water plasticizing coefficient and $\tau_{w,c}$ the coupling coefficient of the permeating component water with the permeating component cyclohexane.

When only the solute swells the top layer, the coupling coefficient can be considered almost negligible (no coupling effects between fluxes of feed components), and the latter equation can be simplified.

$$D_{w,m} = D^0_{w,m} \exp(\tau_{w,w} C^m_w) \quad (5)$$

Thus, integration of Fick's law results in the water flux across the membrane as a function of the concentration difference between both sides of the dense top layer.

$$J_w = \frac{D^0_{w,m}\beta_{w,m}}{\zeta}(C^m_{w,0} - C^m_{w,\zeta}) \quad (6)$$

where

$$\beta_{w,m} = \frac{1}{C^m_{w,0} - C^m_{w,\zeta}} \int \exp(\tau_{w,w} C^m_w)\, dC^m_w \quad (7)$$

Combining Eq. (7) with Eqs. (2) and (3), and neglecting the vapour water concentration at the membrane/permeate interface (again due to low vacuum pressures), water flux can be expressed

as,

$$J_w = \frac{D^0_{w,m}\beta_{w,m}K_{w,0}}{\zeta}C^b_{w,\delta} \quad (8)$$

The influence of water concentration on membrane diffusivity, for dehydration applications at low water contents, can be considered negligible; so it is possible to assume $D_{w,m} \approx D^0_{w,m}$. By doing this, Fick's law integration results in a more simplified expression for description of the water flux across the membrane:

$$J_w = \frac{D^0_{w,m}K_{w,0}}{\zeta}C^b_{w,\delta}. \quad (9)$$

2.3. Mass transport resistances

In order to describe the water flux applying the resistances-in-series model, Eqs. (1) and (6) can be combined in a single expression taking into account both the liquid boundary layer and membrane resistances (R_w); while other resistances, such as those owing to the transport along the porous support or the thin vapour fluid layer present in the permeate side, are considered negligible for low solute contents [13].

$$J_w = \frac{1}{R_{w,L} + R_{w,m}}C^b_{w,0} = \frac{1}{(1/k_l) + \zeta/(D^0_{w,m}\beta_{w,m}K_{w,0})}C^b_{w,0} \quad (10)$$

According to the assumptions considered previously, i.e., thermodynamic equilibrium at the liquid membrane interface and negligible partial pressure of water in the permeate (due to the vacuum applied), the integration of $\beta_{w,m}$ leads to the following expression for the membrane mass transport resistance:

$$R_{w,m} = \frac{\zeta\tau_{w,w}C^b_{w,\delta}}{D^0_{w,m}(\exp(\tau_{w,w}K_{w,0}C^b_{w,\delta}) - 1)} \quad (11)$$

Two characteristic parameters are present in the previous equation, that are needed to predict the solute permeation kinetics,

$$P_1 = \frac{D^0_{w,m}}{\tau_{w,w}}; \qquad P_2 = \tau_{w,w}K_{w,0} \quad (12)$$

where P_1 includes the influence of water diffusivity in the membrane, and P_2 the sorption properties of the materials.

It was mentioned earlier in this paper that a very low swollen membrane leads to a diffusivity in the membrane that is independent of solute concentration; thus, it can be assumed that $\beta_{w,m}$ tends to 1, which is accurate enough for engineering design purposes [10]. Simplification of Eq. (11) leads to the following expression:

$$R_{w,m} = \frac{\zeta}{D^0_{w,m}K_{w,0}} = \frac{\zeta}{P_m} \quad (13)$$

where P_m indicates the membrane permeability to water.

3. Experimental description of the pervaporation unit and membranes used for cyclohexane dehydration

Several pervaporation runs with different membranes were carried out in order to compare their behaviour in the dehydration process. The pervaporation unit, membranes used and experimental methodology followed are described in this section.

3.1. Feed solution

Commercial synthetic cyclohexane with a purity of 99.5% was used in all the experiments to prepare the synthetic feed. The feed was prepared adding the same amount of ultra pure water to the solvent for each run. This provided the same humidity content (75–80 mg/kg) than the industrial cyclohexane to be dehydrated in the synthetic rubber manufacture. Industrial cyclohexane from a synthetic rubber plant was also dehydrated in the experimental pervaporation unit.

3.2. Pervaporation membranes

The behaviour of CMC-CF23, CMC-VP43 and CMC-VP31 hydrophilic membranes, purchased from CM-Celfa (Switzerland), was studied since it was found in the literature that those materials are suitable for dehydration applications; a good description of VP-43 and CF-23 can be found at Gorri et al. [14]. In particular, CF-23 is recommended for the dehydration of organic solvents and consists of an acrylic copolymer top layer protected by a thin coating of a cross-linked polymer blend. Moreover, the porous structure is physically and chemically modified in order to obtain the desired selectivity properties, working as a support on the membrane permeate side. On the other hand, the VP-43 membrane is made of a hydrophilic polymer blend coated onto a porous polyacrylonitrile support, and an additional non-woven structure of polypropylene is incorporated as reinforcement. Then, the active top layer is hereby partially anchored in the substrate pores to improve the membrane mechanical strength. As a result, VP-43 provides high water fluxes at low water temperatures (40–60 °C). The new generation VP-31 membrane is made with the same coating technology as VP-43 in order to allow the application of non-cross-linked and altogether thinner layers. This membrane is also recommended for dehydration of organic solvents, with high permeation nominal fluxes (from 1 to 4.2 kg/m^2 h range) [15], and a water content in the permeate higher than 97%.

Other commercial membranes were analysed in this work; in particular, the hydrophilic Pervap2201 and Pervap2201D membranes, manufactured by Sulzer Chemtech (Germany). Pervap2201 has a cross-linked PVA selective layer and a porous PAN supporting layer cast on a polyphenylene sulphide (PPS) non-woven fabric [16], while Pervap2201D is based on Pervap2201 but with higher cross-linked selective layer, improving the chemical and thermal membrane resistance to specially aggressive organic solvents.

Finally, non-supported homogeneous sulfonated poly(ether ether ketone) (SPEEK) tailor made membranes were kindly supplied by the Membrane Technology Group of the University of

Twente (The Netherlands). In this case, homogeneous hydrophobic poly(ether ether ketone) (PEEK) is reported as an excellent material for its chemical and mechanical properties in aqueous environments. The polymer turns into hydrophilic with a simple and easily controlled sulfonation reaction where higher sulfonation degrees (SD) increment the swelling of the membranes and, thus, their structural stability [17,18]. Although SPEEK membranes are, nowadays, mostly employed in DMFC studies, they

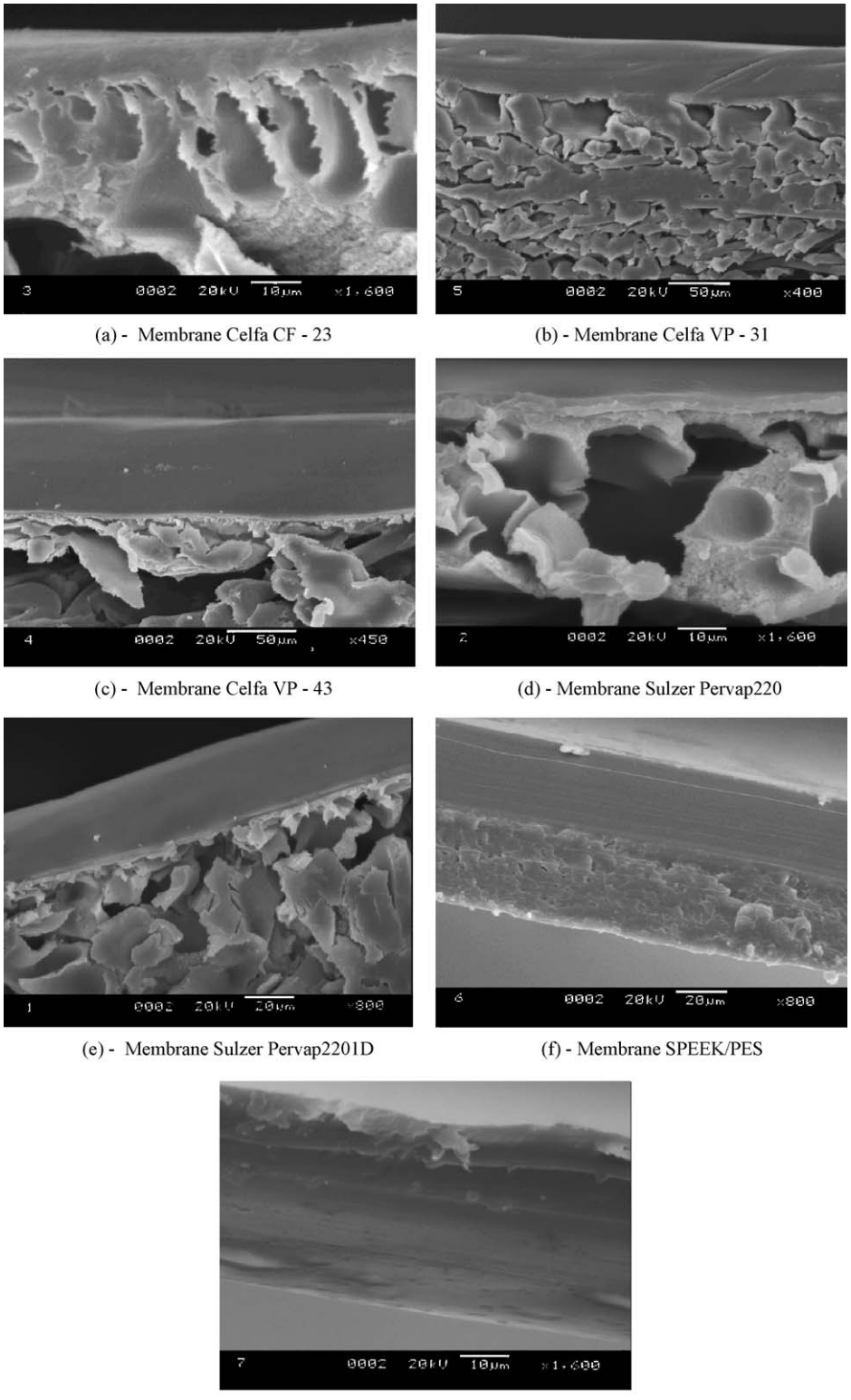

(a) - Membrane Celfa CF - 23

(b) - Membrane Celfa VP - 31

(c) - Membrane Celfa VP - 43

(d) - Membrane Sulzer Pervap220

(e) - Membrane Sulzer Pervap2201D

(f) - Membrane SPEEK/PES

(g) - Membrane SPEEK

Fig. 2. Transversal SEM photographs of all the pervaporation membranes studied. (a) Membrane Celfa CF-23, (b) membrane Celfa VP-31, (c) membrane Celfa VP-43, (d) membrane Sulzer Pervap220, (e) membrane Sulzer Pervap2201D, (f) membrane SPEEK/PES and (f) membrane SPEEK.

have been proposed for dehydration applications by pervaporation as a suitable material at moderate temperatures and water contents in the feed [19].

Thus, higher stability properties can be obtained by blending SPEEK with poly(ether sulfone) (PES). The resultant membrane reduces the excessive swelling of higher sulfonated SPEEK polymers in aqueous mixtures as has been reported previously [20–22]. The same procedure described by Ibáñez et al. [23] was followed in the manufacture of this membrane.

Scanning electron microscope (SEM) pictures of all the pervaporation membranes analysed in this work are presented in Fig. 2, where the support and active layer can be clearly identified in the Celfa and Sulzer membranes, whereas the tailor made ones are unsupported. These pictures were also useful to measure membrane thickness that is reported later.

3.3. Pervaporation unit

The experimental set-up is shown in Fig. 3. Basically, a centrifugal pump is used to recirculate the fluid from the feed jacketed vessel to the pervaporation unit [24]. Then, a membrane cell bypass was implemented in order to obtain enough mixing without mechanical agitation in the feed tank, as well as favouring the water dissolution into cyclohexane before the pervaporation phenomena started. All the experiments were performed at atmospheric pressure in the retentate side; while a needle valve and a vacuum pump (Telstar 2P-3) controlled the permeate side pressure ((2.666448–5.332896) $\times 10^2$ Pa (2–4 mmHg)). The permeate was collected in a cold trap that was cooled using liquid nitrogen. In addition, a sampling valve was installed to collect a few millilitres of fluid at regular intervals of time. The whole pervaporation set-up was made of stainless steel, and all seals were made of Teflon.

All the experiments were performed in a circular plate-and-frame pervaporation test cell made of stainless steel (AISI 316L), as shown in Fig. 4, and circular shaped flat membranes were used providing 179 cm^2 of effective area [24]. Once a sintered metal disc (5 mm width) supported the membrane, the conical cell, where the distance of the plates follows a radial function

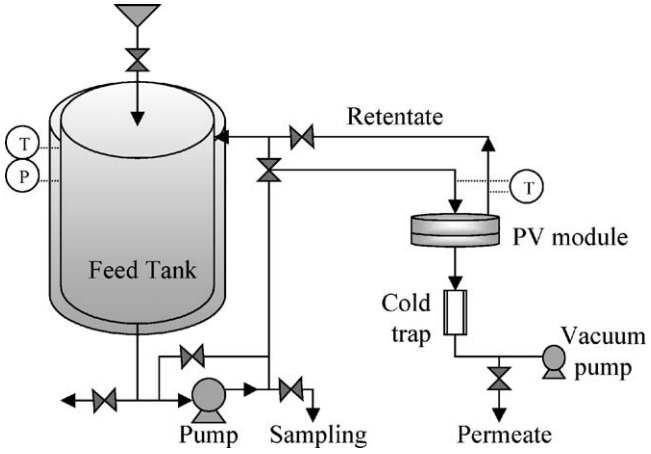

Fig. 3. Schematic diagram of the experimental pervaporation set-up.

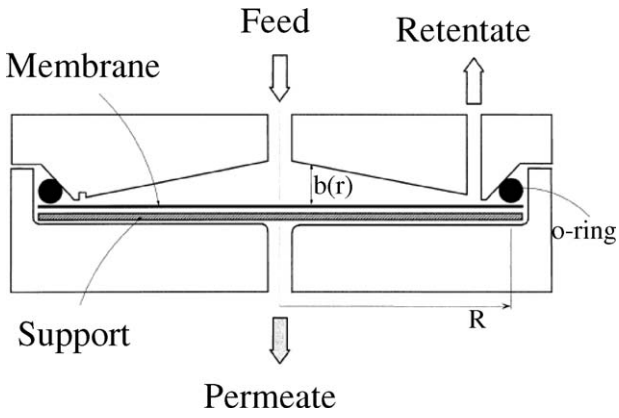

Fig. 4. Pervaporation module.

$b(r)$, was sealed by a fluorelastomeric o-ring. The feed entered through the cell top and after the permeant components had passed across the membrane, they were collected in a cold trap, at the same time that the retentate returned to the feed vessel.

In each experiment, the vessel was filled with 2 l of cyclohexane, and after the desired operation temperature was reached, 0.15 ml of water were added in order to increase the permeant (water) content in the feed while the unit worked in a recycling mode for 2 h to ensure the complete water solution into the tested cyclohexane. Once the experiment started ($t = 0$), 2 ml feed samples were taken every 15 or 30 min, and the permeant content was determined using a Karl Fischer Coulometer (Mettler Toledo DL 36). On the other hand, the permeate was collected in a liquid N_2 cold trap, to be weighted later in a digital balance (Mettler Toledo AB 204-S). A component mass balance was done to confirm the results achieved by comparing the difference of permeant concentration in the feed between the initial and final experimental times to the collected permeate in the cold traps. It is important to remark that the obtained permeate along each experiment consisted of two phases owing to the low mutual solubilities (below 300 mg/kg): a well-defined water drop into a cyclohexane solution. Once the condensed permeate was collected, both phases were separated in order to weight them individually, allowing the evaluation of the membrane selectivity. In addition, the total permeate amount was too small, making it impossible to measure any variation of mass over time without committing an unacceptable error. Thus, only the final permeate was collected.

The operational feed flow rate was 5.3 l/min at 60 °C. Each experiment was duplicated obtaining a standard weighted deviation (σ) lower than 5%. The latter was calculated through Eq. (14), where C_{mes} and C_{av} represent measured and average water concentrations, respectively.

$$\sigma = \sqrt{\frac{\sum_i ((C_{mes,i} - C_{av,i})/C_{mes,i})^2}{N-1}} \quad (14)$$

Finally, a liquid temperature drop of 0.2 °C was observed along the pervaporation cell during the experiments, being an evidence of the permeant phase change involved in the separation process.

4. Results and discussion

4.1. Discussion of the results of cyclohexane dehydration with different membranes

In order to evaluate the behaviour of different pervaporation membranes in the dehydration of cyclohexane process, the evolution of the dimensionless feed water concentration C_w/C_w^0 was studied as a function of time. Results corresponding to experiments at the same operation conditions (5.3 l/min, 60 °C) are shown in Fig. 5, where the vacuum pressure remained constant and equal to ((2.666448–3.999672) × 10^2 Pa (2–3 mmHg)). For the Celfa VP-43 and VP-31, an increase in the vacuum pressure was observed denoting poor membrane stability.

High dehydration kinetics were found when the Celfa membranes were tested, while the results obtained with the non-commercial one – SPEEK/PES – were similar to those obtained with the Sulzer Pervap2201D membrane. As it was mentioned above, accurate measurements of the water condensed in the cold traps was a difficult task; therefore a differential method was applied to the kinetic data "water concentration–time" and the water pervaporation flux was determined ~~by~~ applying Eq. (15), where V, A and ρ represent the feed volume, effective membrane area and water liquid density, respectively.

$$J_w = -\frac{V}{A}\rho\frac{dC_w}{dt} \tag{15}$$

Integration of the latter equation considering a first order law ($J_w = kC_w$) for the flux of water, results in Eq. (16).

$$C_w = C_w^0 \exp\left(-\frac{V}{A}\rho k \cdot t\right) \tag{16}$$

All the experimental data were fitted to an exponential curve, checking the first order kinetic behaviour with a regression coefficient (r) that was above 98%. Finally, the resultant flux values are shown in Fig. 6.

In addition, some experiments were carried out for two more SPEEK type membranes, where the main difference between them was the SD: 50% and 62%. Owing to their tailor made character, the available membrane area was too small to be used in the pervaporation cell previously described; therefore, a smaller (but geometrically identical) cell was used in order to evaluate their separation properties. In this case, the effective area was 51.5 cm^2, and the operation conditions remained the same (5.3 l/min and 60 °C). The two membranes behaved differently although they were made of the same material (SPEEK). The hydrophilic behaviour increases with the degree of sulfonation in the membrane material, as presented in Fig. 7. Together with these data, and in order to take into account the different hydrodynamic conditions between the two cells, experimental work was carried out in the smaller cell using the Celfa VP-43 membrane. Despite the fact that the commercial membrane is more effective for the dehydration process analysed than the SPEEK ones, it showed poor stability, denoted by the vacuum pressure increase and the high flux of cyclohexane observed. Finally, it is shown in Table 1 that the water flux obtained at the beginning of the experiments carried out (maximum water content in the feed) for each membrane tested in both modules.

The selectivity is an important parameter to evaluate the performance of a pervaporation membrane, together with permeability and mechanical and chemical stability. Since an average value of 0.15 g of water was found in every collected permeate, Table 2 shows the water percentage, in the collected permeates.

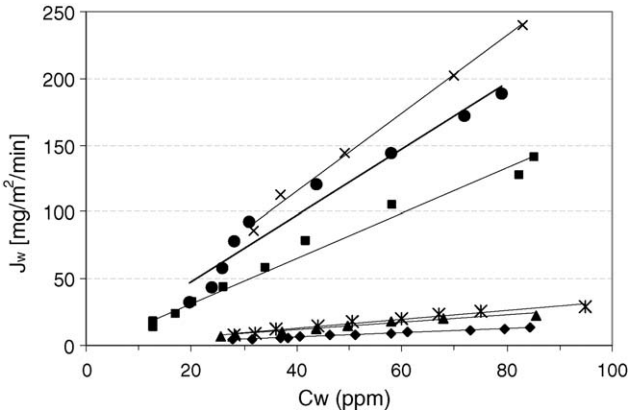

Fig. 6. First order kinetic behaviour of the permeated water flux. (●) Celfa VP-31, (×) Celfa VP-43, (■) Celfa CF-23, (♦) Sulzer Pervap2201, (▲) Sulzer Pervap2201D and (∗) SPEEK/PES.

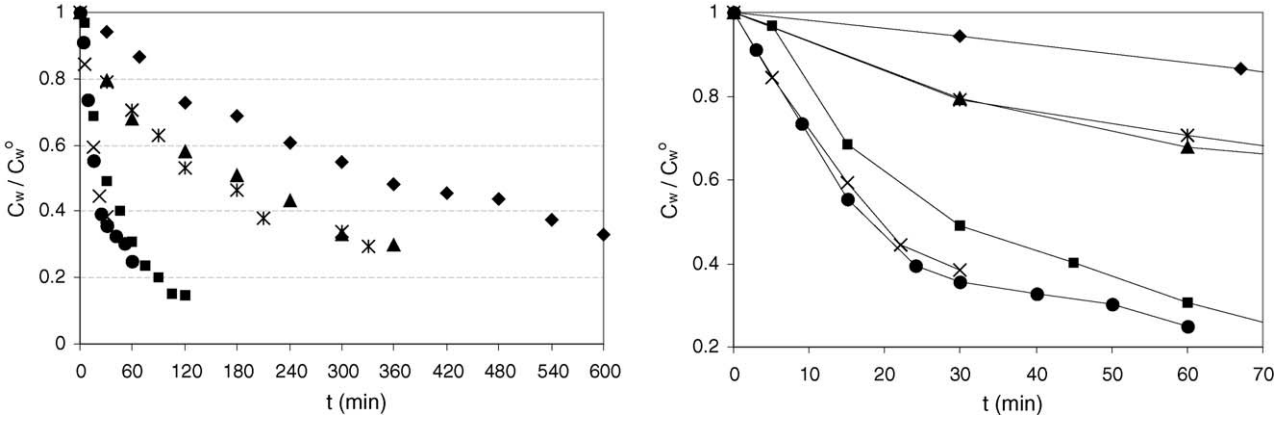

Fig. 5. Dimensionless feed water concentration as a function of time. (●) Celfa VP-31, (×) Celfa VP-43, (■) Celfa CF-23, (♦) Sulzer Pervap2201, (▲) Sulzer Pervap2201D and (∗) SPEEK/PES.

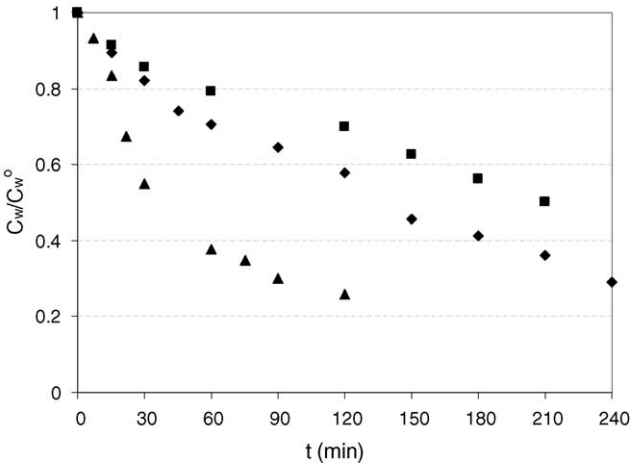

Fig. 7. Dimentionless feed water concentration as a function of time, in a 51.5 cm^2 membrane cell. (■) SPEEK 50%, (♦) SPEEK 62% and (▲) Celfa VP-43.

Table 1
Flux of water obtained at the beginning of the PV experiments

Big module		Small module	
Membrane	J_w (mg/m^2 min)	Membrane	J_w (mg/m^2 min)
CF-23	141	SPEEK 50%	95
VP-31	250	SPEEK 62%	131
VP-43	240	VP-43	382
Pervap2201	13		
Pervap2201D	22		
SPEEK/PES	29		

Thus, Celfa CF-23 and VP-31 membranes, as well as the SPEEK 50% SD, showed an excellent selectivity improving the water mass transport.

Moreover, in order to analyze the feed flow influence over the dehydration rate and to clarify the importance of the concentration polarization phenomenon in the separation process, several experiments (Figs. 8 and 9) were carried out working with different values of feed flow rate at constant temperature (60 °C). As a result, it was found that the liquid layer resistance in the Sulzer Pervap2201D is smaller than the resistance offered by the membrane itself, since the standard deviation found was 3.90% when the minimum and maximum flow rate – allowed by the pump – were applied. On the other hand, the opposite phenomenon could be observed with the Celfa CF-23 membrane,

Table 2
Water percentage present in the collected permeate working with different membranes

Membrane	Water (wt.%)
CF-23	≈100.00
VP-31	≈100.00
VP-43	3.21
Pervap2201	26.90
Pervap2201D	15.27
SPEEK/PES	0.27
SPEEK 50%	≈100.00
SPEEK 62%	13.03

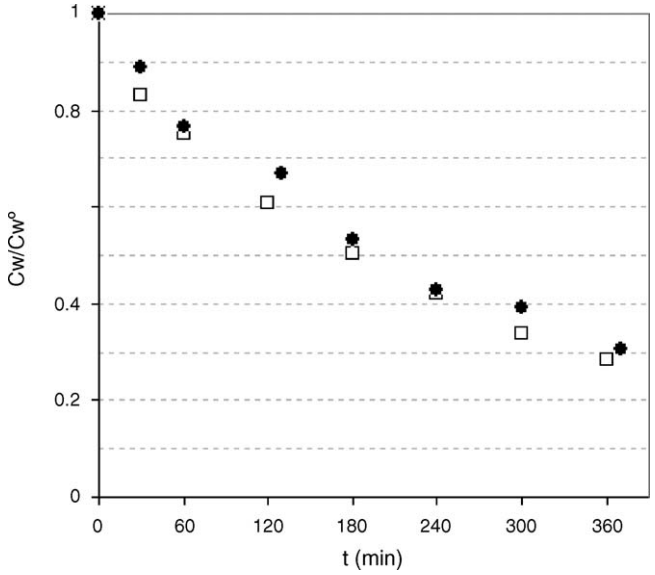

Fig. 8. Feed flow influence over mass transfer using the pervaporation Sulzer Pervap2201D membrane. (●) 2.5 l/min, (□) 5.3 l/min and $\sigma = 3.90\%$.

where the feed flow rate clearly affected the separation task with a standard deviation of 10.77%.

4.2. Estimation of water permeability, liquid layer and membrane resistances for different membranes

Experimental results obtained with different membranes were employed in the estimation of the membrane resistance influence over the water mass transport. The mathematical model, including mass balances within the pervaporation plant and cell geometry, was implemented in gPROMS®. It was found in the literature that the hydrodynamic influence over the boundary layer resistance in conical cells could be well defined by using a 0.81 value in the empirical correlation for the calcula-

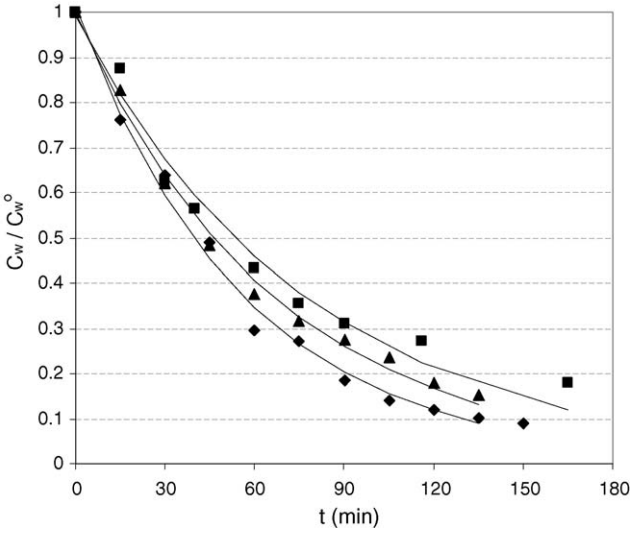

Fig. 9. Feed flow influence over mass transfer using the pervaporation Celfa CF-23 membrane. (■) 2.5 l/min, (▲) 4.0 l/min, (♦) 5.3 l/min and $\sigma = 10.77\%$ (between minimum and maximum flow rates).

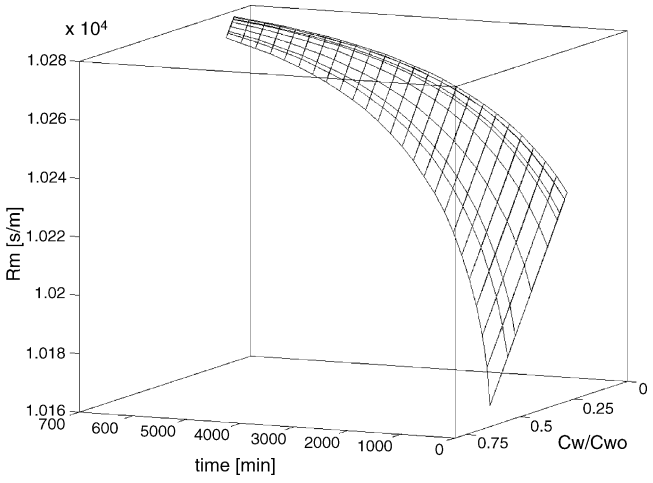

Fig. 10. Membrane resistance as a function of the dimensionless water content at the liquid/membrane interface, over time.

tion of k_l in Eq. (1), where Sherwood, Reynolds and Schmidt numbers were dependent of the cell radius [24],

$$Sh(r) = 0.81 Re(r)^{0.5} Sc^{0.33} \quad (17)$$

The water mass transport across the membrane was initially modelled assuming a concentration dependence of the diffusivity (Eq. (8)), where parameters P_1 and P_2 were estimated from the experimental data obtained for each membrane using the gEST tool of gPROMS® by means of the experimental data obtained for each membrane. Fig. 10 shows the relation between the calculated water concentration at the liquid/membrane interface, $C^{b}_{w,\delta}$, and the calculated membrane resistance for the Celfa CF-23. As expected for the low water content in the feed, the solute concentration influence over the membrane resistance results negligible, implying that $\beta_{w,m}$ is close to unity owing to the low swelling of the membrane. Therefore, Eq. (9) should describe the water transport across the top layer satisfactorily. Similar results were found for the rest of the membranes analysed.

The experimental data were used again in the estimation of the membrane contribution to the overall water mass transport resistance, using the simplified model described earlier. Fig. 11 shows graphically the results of the relative influence of both resistances (the liquid boundary layer and the membrane itself) over the mass transport kinetics for each studied membrane. As it can be seen, the liquid film layer resistance is only important in the dehydration process in the case of the CM-Celfa materials, being the membrane resistance contribution slightly significant only for the commercial CF-23 membrane. These results are consistent with the experimental behaviour observed in Figs. 8 and 9. The opposite result is obtained for the rest of the commercial and tailor-made membranes tested, where only SPEEK samples presented a more balanced contribution of both resistances.

Table 3
Liquid layer and membrane resistance quantification and the permeability parameters obtained using the mathematical model proposed in this paper

Membrane	Thickness (ζ) (μm)	R_l (s/m)	R_m (s/m)	Permeability (m^2/s)
CF-23	7	1.87E4	6.25E3	1.12E
VP-31	50	1.87E4	Negligible	–
VP-43	72	1.87E4	Negligible	–
Pervap2201	8	1.87E4	2.5E5	3.21E−11
Pervap2201D	33	1.87E4	1.13E5	2.92E−10
SPEEK/PES	70	1.87E4	8.05E4	8.70E−10
SPEEK 50%	45	1.13E4	3.7E4	1.22E−09
SPEEK 62%	45	1.13E4	1.96E4	2.29E−09

Normalized water permeability values were calculated, applying the simplified model discussed above using the membrane resistances and the dense top layer thickness estimated from the SEM photographs reported in this work. Table 3 shows the membranes thickness, mass transport resistances and permeability values for the membranes analyzed in this work. Promising results were found with SPEEK materials. As it was expected, higher sulfonation degrees incremented the hydrophilic character of the polymer obtaining good permeability values in the range of the water concentration studied. In the case of the SPEEK/PES blend material, hydrophobic properties of PES produced a significant decrease of the polymer dehydration capacity, being its permeability value in the range of the values obtained for the Sulzer samples. Commercial CM-Celfa polymers resulted the most suitable materials for dehydration purposes in the range of the feed water concentrations studied although membranes of the VP series presented poor chemical stability towards cyclohexane. CF-23 Celfa membrane presented good chemical and physical stability indicating its suitability for industrial applications.

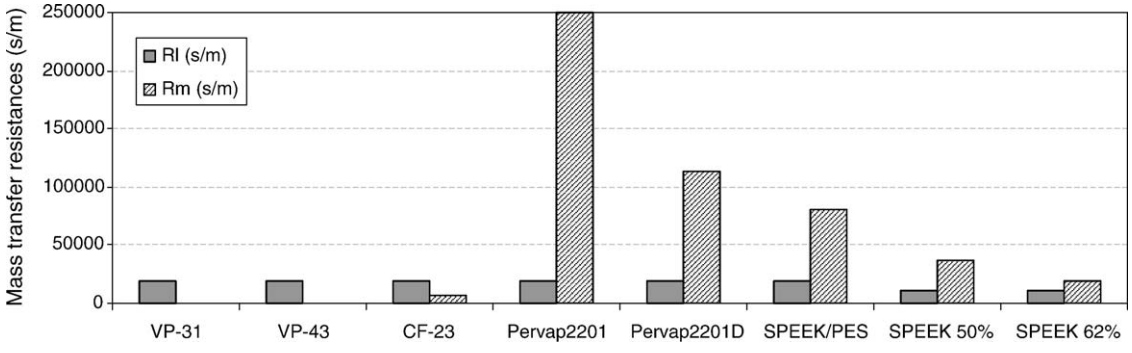

Fig. 11. Relative importance of mass transport resistances over the dehydration process, assuming constant diffusivity through the membrane, at 60 °C.

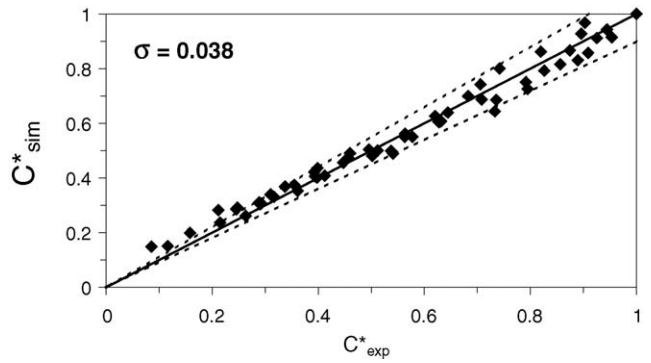

Fig. 12. Parity graph of the adimensional water concentrations for all the membranes studied. C^*_{sim} and C^*_{exp} represent the simulated and experimental water concentration, respectively.

The accuracy of the simulation results is presented through the parity graph shown in Fig. 12. The predicted water concentration values, C^*_{sim}, are represented versus the experimental data, C^*_{exp}, for the membranes studied in this work. Ninety percent of the results of C^*_{sim} fall within the interval $C^*_{exp} \pm 10\% C^*_{exp}$, resulting in a standard deviation below 4% and proving that the model proposed describes satisfactorily well the water mass transport. The highest error observed corresponded to the lower water contents, where the analytical techniques employed were less precise.

Finally, industrial cyclohexane was received from a synthetic rubber plant and was dehydrated in order to validate the model and parameters reported. The solvent contained small amount of impurities, such as butadiene, 2- and 3-methyl-pentane and *n*-hexane. In order to evaluate the accuracy of the results for design purposes, pervaporation experiments with synthetic and industrial cyclohexane were carried out at similar operating conditions. The results obtained showed a standard weighted deviation below 5% (see Fig. 13) that remains in the range of the accuracy found for the analytical techniques used. Thus, the model and parameters reported can be applied for the dehydration of the industrial solvent.

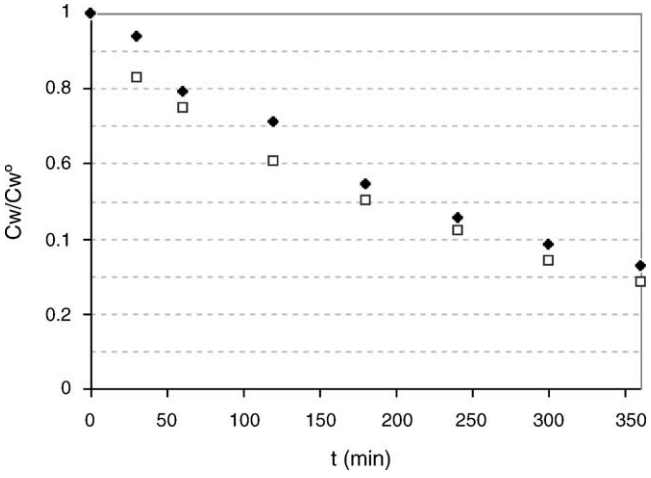

Fig. 13. Dimensionless feed water concentration for the dehydration of (□) synthetic and (●) industrial cyclohexane using a Sulzer Pervap2201D membrane, for 5.3 l/min feed flow and 60 °C.

5. Conclusions

The behaviour of commercial and tailor-made membranes in the pervaporative dehydration of cyclohexane, commonly used as solvent in the synthetic rubber industry, has been studied in this work.

Commercial Celfa CF-23 membrane presented good selectivity, permeability and satisfactory mechanical and chemical resistance (constant vacuum pressure along the experiments. It has also the best performance in terms of dehydration removing 85% of water. On the other hand, SPEEK tailor made membranes showed a similar behaviour, becoming an interesting option for this purpose. In addition, a supported SPEEK membrane would lead to a smaller membrane thickness, reducing the membrane resistance and increasing the permeate flux.

Taking into account only the permeability and selectivity of the membranes, the Celfa VP seems to be the most adequate membrane in order to carry out the pervaporation at 60 °C. However, during the experiments an increase in the vacuum pressure was observed, indicating some lack of chemical and/or mechanical stability; a short lifetime could lead to a significant increase in the membrane replacement costs.

In addition, the Sulzer membranes tested showed poor separation properties in the range of the feed water concentration studied, since they are not as selective as the others at the same time that their permeability remains too small. Finally, SPEEK/PES materials behaved similarly to the commercial Pervap membranes.

The mathematical model of the pervaporation process that accounts for the liquid layer and membrane resistances, and the corresponding parameters such as water permeability and membrane thickness, are reported for several commercial and tailor-made membranes studied. The model and parameters have been validated with experimental data dehydrating synthetic and industrial cyclohexane.

As a result, this work provides the information needed of the behaviour of PV membranes for dehydration of industrial cyclohexane, reporting the water mass transport properties of the studied materials, needed for design purposes.

Acknowledgements

This work would not have been possible without the financial support given by several sources. Authors thank the Programme Alβan (Scholarship No. E04D037382AR), Fundación Antorchas, CICYT projects BQU2002-03357 and PTR1995-0588-OP for their economic support.

In addition, the invaluable collaboration of the Membrane Technology Group of the University of Twente, The Netherlands, is also gratefully recognized.

Nomenclature

A	membrane effective area (m^2)
C	liquid concentration (mg/kg = ppm)
D	diffusion coefficient of water in the membrane (m^2/s)
D^0	intrinsic diffusion coefficient of water in the membrane (m^2/s)
J	permeate flux (mg/m^2 min)
k_l	liquid boundary layer mass transfer coefficient (m/s)
$K_{w,0}$	sorption coefficient of water
$K_{w,\zeta}$	desorption coefficient of water
P_m	membrane permeability (m^2/s)
R_m	mass transport membrane resistance (s/m)
R_l	mass transport liquid layer resistance (s/m)
Re	Reynolds number on feed side
Sc	Schmidt number on feed side
Sh	Sherwood number on feed side
t	time (min)
V	feed vessel volume (m^3)

Greek letters

$\beta_{w,m}$	enhancement factor to diffusion coefficient
δ	liquid boundary layer thickness (m)
γ	activity coefficient
ρ	mass liquid density (kg/m^3)
σ	standard weighted deviation
ζ	membrane thickness (m)
$\tau_{w,c}$	coupling coefficient of water with component cyclohexane
$\tau_{w,w}$	water plasticizing coefficient

Subscripts

c	cyclohexane
w	water

Superscripts

b	in the liquid side (bulk)
m	within the membrane
o	initial condition
p	in the permeate side

References

[1] F. Ullmann (Ed.), Ullmann's Encyclopedia of Industrial Chemistry, sixth ed., Wiley–VCH, 1999 (Electronic Release).

[2] Kirk-Othmer (Ed.), Encyclopedia of Chemical Technology, Wiley & Sons Inc., 1984.

[3] R.Y.M. Huang, Pervaporation Membrane Separation Processes, Elsevier, Amsterdam, 1991.

[4] A. Jonquières, R. Clément, P. Lochon, J. Néel, M. Dresch, B. Chrétien, Industrial state-of-the-art of pervaporation and vapour permeation in the western countries, J. Membr. Sci. 206 (2002) 87–117.

[5] H.E.A. Brüschke, State of the art of pervaporation processes in the chemical industry, in: S.P. Nunes, K.-V. Peinemann (Eds.), Membrane Technology in the Chemical Industry, Wiley–VCH, Weinheim, 2001.

[6] J. Li, C. Chen, B. Han, Y. Peng, J. Zou, W. Jiang, Laboratory and pilot-scale study on dehydration of benzene by pervaporation, J. Membr. Sci. 203 (2002) 127–136.

[7] I. Ortiz, A. Urtiaga, R. Ibáñez, P. Gómez, D. Gorri, Laboratory and pilot plant study on dehydration of cyclohexane by pervaporation, J. Chem. Technol. Biotechnol. 81 (2006) 48–57.

[8] A.S. Michaels, Effects of feed-side solute polarization on pervaporative stripping of volatile organic solutes from dilute aqueous solution: a generalized analytical treatment, J. Membr. Sci. 101 (1995) 117–126.

[9] B. Raghunath, S.-T. Hwang, Effect of boundary layer mass transfer resistance in the pervaporation of dilute organics, J. Membr. Sci. 65 (1992) 147–161.

[10] M.G. Liu, J.M. Dickson, P. Côté, Simulation of a pervaporation system on the industrial scale for water treatment. Part I: extended resistance-in-series model, J. Membr. Sci. 111 (1996) 227–241.

[11] R. Jiraratananon, A. Chanachai, R.Y.M. Huang, Pervaporation dehydration of ethanol-water mixtures with chitosan/hydroxyethylcellulose (CS/HEC) composite membranes II. Analysis of mass transport, J. Membr. Sci. 199 (2002) 211–222.

[12] M. Mulder, Basic Principles of Membrane Technology, Kluwer Academic Publishers, Dordrecht, 1996.

[13] M. She, S.-T. Hwang, Concentration of dilute flavor compounds by pervaporation: permeate pressure effect and boundary layer resistance modelling, J. Membr. Sci 236 (2004) 193–202.

[14] D. Gorri, A. Urtiaga, I. Ortiz, Pervaporative recovery of acetic acid from an acetylation industrial effluent using commercial membranes, Ind. Eng. Chem. Res. 44 (2005) 977–985.

[15] CM-Celfa Membrantrenntechnik, Technical Data Sheets, PD52D1003.

[16] X. Qiao, T.-S. Chung, W.F. Guo, T. Matsuura, M.M. Teoh, Dehydration of isopropanol and its comparison with dehydration of butanol isomers from thermodynamic and molecular aspects, J. Membr. Sci. 252 (2005) 37–49.

[17] J. Balster, O. Krupenko, I. Pünt, D.F. Stamatialis, M. Wessling, Preparation and characterization of monovalent ion selective cation exchange membranes based on sulfonated poly(ether ether ketone), J. Membr. Sci. 263 (2005) 137–145.

[18] R.Y.M. Huang, P. Shao, C.M. Burns, X. Feng, Sulfonation of poly(ether ether ketone): kinetic study and characterization, J. Appl. Polym. Sci. 82 (2001) 2651–2660.

[19] R.Y.M. Huang, Pinghai Shao, X. Feng, C.M. Burns, Pervaporation separation of water/isopropanol mixture using sulfonated poly(ether ether ketone) (SPEEK) membranes: transport mechanism and separation performance, J. Membr. Sci. 192 (2001) 115–127.

[20] K.D. Kreuer, On the development of proton conducting polymer membranes for hydrogen and methanol fuel cells, J. Membr. Sci. 185 (2001) 29–39.

[21] C. Manea, M. Mulder, Characterization of polymer blends of polyethersulfone/sulfonated polysulfone and polyethersulfone/sulfonated polyetheretherketone for direct methanol fuel cell applications, J. Membr. Sci. 206 (2002) 443–453.

[22] S. Swier, V. Ramani, J.M. Fenton, H.R. Kunz, M.T. Shaw, R.A. Weiss, Polymer blends based on sulfonated poly(ether ketone ketone) and poly(ether sulfone) as proton exchange membranes for fuel cells, J. Membr. Sci. 256 (2005) 122–133.

[23] R. Ibañez, D.F. Stamatialis, M. Wessling, Role of membrane surface in concentration polarization at cation exchange membranes, J. Membr. Sci. 239 (2004) 119–128.

[24] A.M. Urtiaga, E.D. Gorri, I. Ortiz, Modeling of the concentration-polarization effects in a pervaporation cell with radial flow, Sep. Purif. Technol. 17 (1999) 41–51.